九州大学学術情報リポジトリ
Kyushu University Institutional Repository

Long Waves Generated by Topography in Two-Layer Fluid with Infinite Depth-Forced Benjamin-Ono Equation

Tsuji, Hidekazu
Research Institute for Applied Mechanics, Kyushu University

Inada, Manabu
Department of Earth System and Technology, Interdisciplinary Graduate School of Engineering Sciences, Kyushu University

Oikawa, Masayuki
Research Institute for Applied Mechanics, Kyushu University

https://doi.org/10.15017/17450

出版情報：九州大学大学院総合理工学報告. 19 (3), pp.331-337, 1997-12-01. 九州大学大学院総合理工学研究科
バージョン：
権利関係：

九州大学大学院総合理工学研究科報告
第19巻 第3号 331 - 337頁 平成9年12月

Engineering Sciences Reports, Kyushu University
(KYUSHU DAIGAKU SOGORIKOGAKU KENKYUKA HOKOKU)
Vol. 19, No. 3 pp. 331 - 337 DEC. 1997

Long Waves Generated by Topography in Two-Layer Fluid with Infinite Depth — Forced Benjamin-Ono Equation

Hidekazu TSUJI*, Manabu INADA** and Masayuki OIKAWA*

(Received August 31, 1997)

Weakly nonlinear long waves generated by topography in a uniform flow of two-layer fluid in which one layer has infinite depth are considered. They are described by a forced Benjamin-Ono (fBO) equation when the linear wave speed is close to the uniform flow speed. Generation and propagation of waves are investigated by solving the fBO equation numerically for various flow speed and topography. Approximate analysis is possible for the topography with very small (or large) steepness. Its results are compared with the numerical results.

1. Introduction

There are many works on wave generation through interaction between flow and topography in a stratified fluid. Some of them deal with a two-layer fluid model because of its simplicity.

Linear analysis shows that if the linear wave speed is close to the flow speed, resonance occurs and nonlinear analysis is inevitable [1]. In weakly nonlinear analysis, the fundamental equations and boundary conditions can be reduced to a simple model equation. This has different form depending on the horizontal and vertical scales of the system. If the characteristic horizontal length is much longer than the depth of the fluid, the motion is described by the forced Korteweg-de Vries (fKdV) equation [1] or by the forced extended Korteweg-de Vries equation [2]. On the other hand, if the fluid includes a layer which has the vertical scale much longer than the characteristic horizontal length, a forced Benjamin-Ono (fBO) equation [5] is derived. This is the BO equation [3,4] with an forcing term due to topography. Recently, Matsuno [5] investigated analytically interaction of a solitary wave with topography using this equation.

In this paper we solve the fBO equation numerically to investigate resonant generation of waves by the topography in the uniform incident flow. It is noted that Grimshaw [6] also investigated the fBO equation, which was derived from shallow water equations of a rotating fluid. The equation can be simplified and approximate analysis is possible, on condition that steepness of the topography is very small or large. Its results are compared with the numerical results.

In Section 2 the setting of the problem and the fBO equation are briefly explained. Section 3 is devoted to the numerical results, approximate analysis and discussion. Finally conclusion is given in Section 4.

2. Setting of the problem and the fBO equation

Consider an inviscid incompressible two-layer fluid system (**Fig. 1**). Suppose that the flow at $x' \to \infty$ has uniform velocity $(U, 0)$; so in each of two layers flow is irrotational everywhere and velocity potential can be defined. In the vertical direction, the upper layer extends to infinity, while the lower layer has local bottom topography $z' = -h + B'(x)$ ($B' \to 0$ as $|x'| \to \infty$). The interface between two layers is described by $z' = \zeta'(x', t')$ and at initial instant $(t' = 0)$ equals to zero everywhere. The density of the upper fluid is ρ_1 and that of lower fluid is ρ_2.

*Research Institute for Applied Mechanics, Department of Earth System Science & Technology
**Graduate Student, Department of Earth System Science & Technology

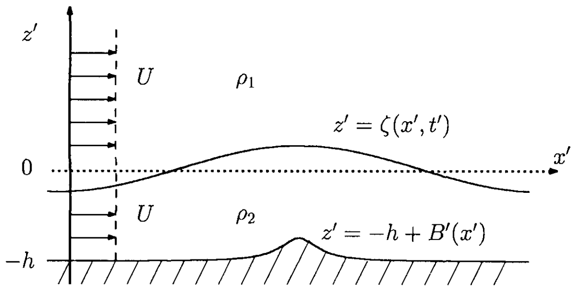

Fig. 1　Two-layer fluid.

The fundamental equations are Laplace's equations together with the boundary conditions at the interface, the bottom and $z' \rightarrow \infty$. Here we introduce a characteristic wave amplitude a, a characteristic horizontal length l and the maximum of the topography B_m. Suppose the following relations

$$\epsilon \equiv \frac{a}{h} \ll 1,\ \ \delta \equiv \frac{h}{l} \sim \epsilon,\ \beta \equiv \frac{B_m}{h} \sim \epsilon^2.$$

The Froude number is defined by $F \equiv U/V$, where $V = \sqrt{(1-\Delta)gh}$ is the phase speed of linear long wave, g is the gravitational acceleration and Δ is density ratio ρ_1/ρ_2. In order to investigate the resonant case, assume that $F = 1 + \epsilon\Gamma$.

Expanding the fundamental equations and boundary conditions in series of ε, we obtain the equation:

$$\frac{\partial \zeta}{\partial t} + \Gamma \frac{\partial \zeta}{\partial x} - \frac{3}{2}\zeta \frac{\partial \zeta}{\partial x} - \frac{\delta}{2\epsilon}\Delta \mathcal{H}\left[\frac{\partial^2 \zeta}{\partial x^2}\right] = \frac{\beta}{2\epsilon^2}\frac{\partial B}{\partial x},$$

where $x = x'/l$, $B = B'/B_m$ and ζ is the leading order of ζ'/a, and $t = (\epsilon V/l)t'$, which means the equation describes long-time behavior of wave motion. The notation $\mathcal{H}$ denotes the Hilbert transform :

$$\mathcal{H}\left[f(x)\right] = \frac{1}{\pi} \mathrm{P} \int_{-\infty}^{\infty} \frac{f(y)}{y-x} dy,$$

where P stands for Cauchy's principal value.

For simplicity, using the transformations $\zeta = (8/3)\eta$, $x = (\delta/2\epsilon)\Delta\xi$, $t = (\delta/2\epsilon)\Delta\tau$ and $B = (16\epsilon^2/3\beta)H$, the equation is reduced to

$$\frac{\partial \eta}{\partial \tau} + \Gamma \frac{\partial \eta}{\partial \xi} - 4\eta \frac{\partial \eta}{\partial \xi} - \mathcal{H}\left[\frac{\partial^2 \eta}{\partial \xi^2}\right] = \frac{\partial H}{\partial \xi}. \tag{1}$$

This form of fBO equation is hereafter used.

It is noted that without forcing $H = 0$, the equation has the N-soliton solutions. For $N = 1$, the form is

$$\eta = \frac{A}{A^2[\xi + (A-\Gamma)\tau]^2 + 1}, \tag{2}$$

where A is a parameter.

In the following discussion, the topography is given by

$$H = \frac{H_m}{(b\xi)^2 + 1}, \tag{3}$$

where H_m is constant and the parameter b gives a measure of steepness of the topography. In what follows, we take $H_m = 1$ without loss of generality. Since the maximum of B is 1, this means that we should take $\epsilon = \sqrt{3\beta}/4$.

The numerical scheme for solving the equation is an implicit spectral method [7]. Note that the Fourier coefficients of the Hilbert transform are approximated as $i\,\mathrm{sgn}(k)c_k$ where k is wave number and c_k is the Fourier coefficients of η. These are based on the Fourier transform of the Hilbert transform. Our initial condition is that there is no wave in the fluid at $\tau \leq 0$ and at $\tau =$

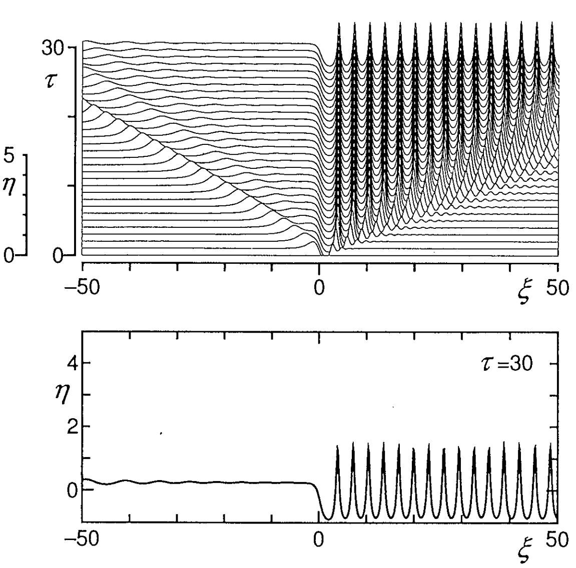

Fig. 2 Generation and propagation of the interfacial waves. $\Gamma = -2$, $b = 1$.

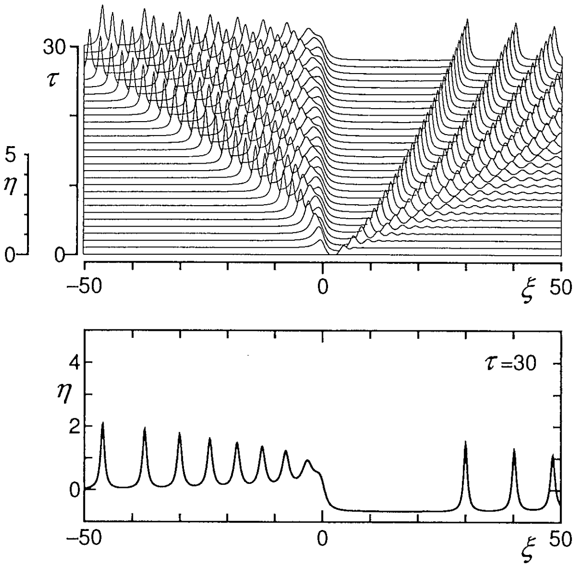

Fig. 3 Generation and propagation of the interfacial waves. $\Gamma = 0$, $b = 1$.

0 the topography suddenly appears.

3. Result and discussion

3.1 Dependence on Froude number

First, generation and propagation of the interfacial waves for several values of Γ is shown in order to clarify its dependence on the Froude number. The results for $b = 1$ are chosen as a typical example.

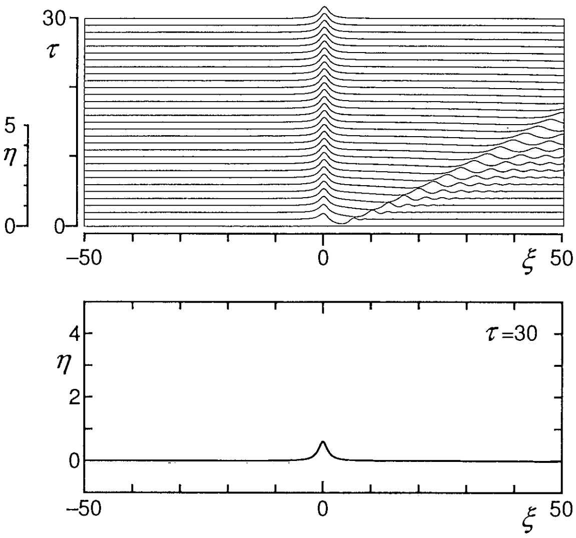

Fig. 4 Generation and propagation of the interfacial waves. $\Gamma = 2$, $b = 1$.

Figure 2 shows the result for $\Gamma = -2$. On the upstream side of the topography, a hump is formed initially due to the obstruction and grows in time. When its amplitude attains to a certain value, it starts to move upstream and is followed by smaller wave tail. After the waves are emitted, the interface settles to an almost constant state with a positive value in the vicinity of the topography. On the downstream side, a wave train with larger amplitude is formed. It extends from the vicinity of the topography, and there a steady solitary wave train is formed eventually.

Figure 3 shows the result for $\Gamma = 0$, which is exactly the resonant case. On the upstream side of the topography, a train of solitary waves can be seen. Near the topography a small wave is emitted upstream and grows up to a solitary wave. The amplitude of the wave is larger than that for $\Gamma = -2$. The speed of the soliton solution is proportional to its amplitude (see (2)), so the larger amplitude is required for the solitary wave to propagate upstream against larger speed of uniform flow. On the downstream side, the uniform depression can be seen near the topography. It is followed by a modulated solitary wave train and extends as the solitary waves go downstream.

The result for $\Gamma = 2$ (large positive Γ) is shown in **Fig. 4**. There is no wave on the upstream side of the topography. Moreover, except that an initial transient disturbance propagates downstream, no wave is recognized also on the downstream side of the topography. Only a steady hump above the topography can be seen.

Figure 5 shows an intermediate state between those of **Fig. 3** and **Fig. 4**. It is the case of $\Gamma = 1.8$, in which qualitative nature is close to that of $\Gamma = 0$. Because of the stronger uniform flow, the solitary waves emitted upstream must have larger amplitudes and the frequency of emission is lower than that of the case of $\Gamma = 0$. On the downstream side of the topography, both formation of uniform depression and that of a solitary wave train are not obvious. A small disturbance is emitted to downstream associated with the formation of solitary wave moving upstream.

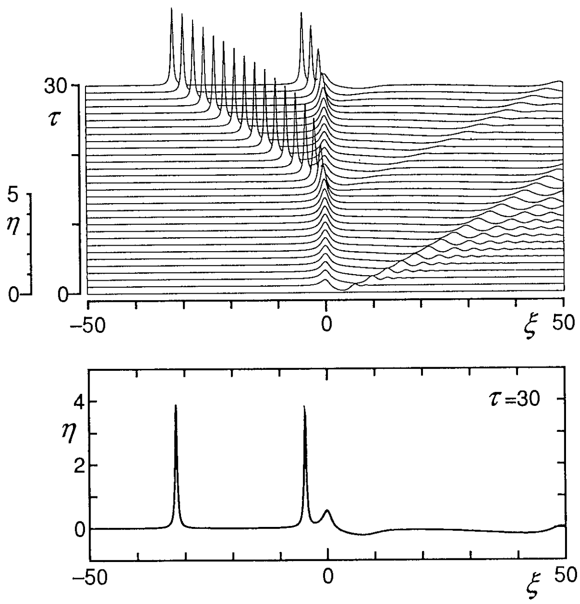

Fig. 5 Generation and propagation of the interfacial waves. $\Gamma = 1.8$, $b = 1$.

3.2 Comparison with analytical result

Useful approximations for eq. (1) are possible in two cases: $b \ll 1$ and $b \gg 1$. The analytical results are obtained in approaches similar to those done by Grimshaw and Smyth [1] for the fKdV equation.

3.2.1. $b \ll 1$

Using the transformation $X = b\xi$, $T = b\tau$ and the topography (3), eq. (1) is reduced to

$$\frac{\partial \eta}{\partial T} + \Gamma \frac{\partial \eta}{\partial X} - 4\eta \frac{\partial \eta}{\partial X} - b\,\mathcal{H}\left[\frac{\partial^2 \eta}{\partial X^2}\right] = \frac{\partial H}{\partial X}.$$

If the wave steepness is not large, we can neglect the dispersive term to obtain

$$\frac{\partial \eta}{\partial T} + \Gamma \frac{\partial \eta}{\partial X} - 4\eta \frac{\partial \eta}{\partial X} = \frac{\partial H}{\partial X}. \tag{4}$$

This can be analyzed by the method of characteristics. The result depends on Γ.

In the case that $|\Gamma| < \sqrt{8}$, two jumps are expected in the flow. One is formed for $X < 0$ and propagates to $X = -\infty$, and the other for $X > 0$ and to $X = \infty$. Eventually η between the jumps is well approximated by

$$\eta(X) = \begin{cases} \dfrac{\Gamma - \sqrt{8(1-H(X))}}{4}, & X \geq 0, \\ \dfrac{\Gamma + \sqrt{8(1-H(X))}}{4}, & X \leq 0, \end{cases} \tag{5}$$

We denote the height of the jump in $X > 0 (<0)$ as $\eta_+ (\eta_-)$:

$$\eta_\pm = \frac{\Gamma \mp \sqrt{8}}{4}, \tag{6}$$

which is obtained by taking $H(X) = 0$. Noto that $\eta_+ < 0$ and $\eta_- > 0$.

On the other hand, $|\Gamma| > \sqrt{8}$, there is no jump and the final steady state is

$$\eta = \frac{1}{4}\left(\Gamma - \mathrm{sgn}(\Gamma)\sqrt{\Gamma^2 - H(X)}\right), \quad |\Gamma| > \sqrt{8}, \tag{7}$$

that is, a hump (depression) above the topography for $\Gamma > 0$ (< 0) and vanishes at $|X| \to \infty$. In practice, as a result of mass conservation, there is additional disturbance moving downstream (upstream) for $\Gamma > 0$ (< 0).

3.2.2. $b \gg 1$

In this case $H(x)$ can be approximated by means of the delta function (see (3)). Steady state is assumed then eq.(1) is

$$\Gamma \frac{\partial \eta}{\partial \xi} - 4\eta \frac{\partial \eta}{\partial \xi} - \mathcal{H}\left[\frac{\partial^2 \eta}{\partial \xi^2}\right] = \frac{\partial}{\partial \xi}\left(\frac{\pi}{b}\delta(\xi)\right), \tag{8}$$

where the factor π/b is defined so that $\int H(\xi)d\xi$ is conserved. Unlike the fKdV equation [1], this equation is more difficult to solve even the steady state is considered. So form of solution is assumed in advance.

Suppose that two cases exist depending on the magnitude of Γ. Note that it is justified later in the derivation.

One case is for small Γ and the solution of the form (a steady solitary wave + constant) is assumed for each of $\xi < 0$ and $\xi > 0$. Then it is found that the wave profile consists of a constant elevation η_- with a solitary wave for $\xi < 0$ and a constant depression η_+ without solitary wave for $\xi > 0$. The values of $\eta_\pm$ are

$$\eta_\pm = \frac{1}{2}\left(\mp \frac{\pi}{b} + \frac{\Gamma}{2}\right), \tag{9}$$

and it is valid on condition that $|\Gamma| < 2\pi/b$.

The other is for large Γ and assume that there is a hump above the topography. Then its form is derived:

$$\eta = \frac{\Gamma}{\Gamma^2(\xi \pm \xi_1)^2 + 1}, \tag{10}$$

where ξ_1 is the larger root of $\xi_1^2 - (2b/\pi)\xi_1 + 1/\Gamma^2 = 0$. It is valid on condition that $|\Gamma| > 2\pi/b$, so simplified analytical solutions are obtained for the whole range of Γ.

It is noted here that, in reality, modulated wave trains exist between the quiescent region away from the topography and the steady non-zero elevation or depression $\eta_\pm$ near the topography. In the corresponding situations in the analysis of the fKdV equation, Grimshaw and Smyth [1] used a modulated cnoidal wave solution of the KdV equation. The similar approach for the fBO equation appears to be difficult because of its complicated dispersive term.

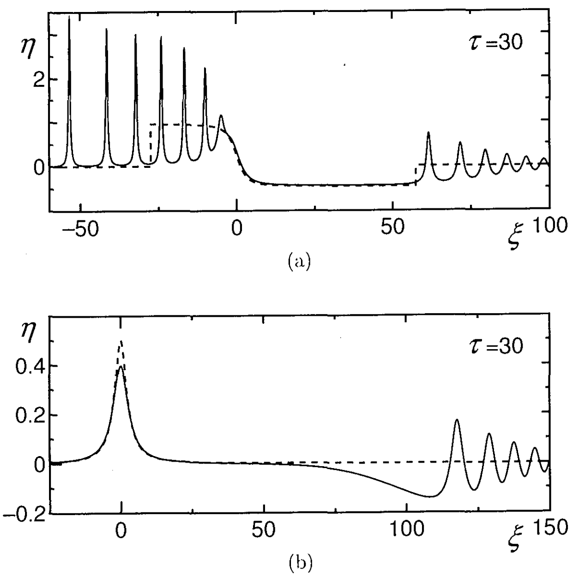

Fig. 6 Generation and propagation of the interfacial waves. $b = 0.3$ and $\tau = 30$. (a) $\Gamma = 1$, (b) $\Gamma = 3$. Solid line shows the result of numerical calculation, dashed line the analytical one for $b \ll 1$.

3.2.3 Comparison

First the profiles are compared. **Figure 6(a)** is the case of $\Gamma = 1$. This is an example of small Γ : $\Gamma < 2\sqrt{2}$. The solid line denotes the numerical solution and the dashed line the formula (5). The locations of the jumps are approximate ones which are given

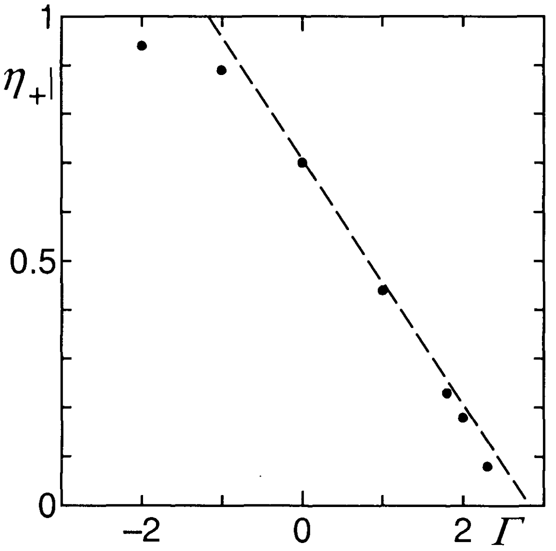

Fig. 7 The change in the depression $|\eta_+|$ with varying Γ. $b = 0.3$. Dashed line is the approximated solution for $b \ll 1$.

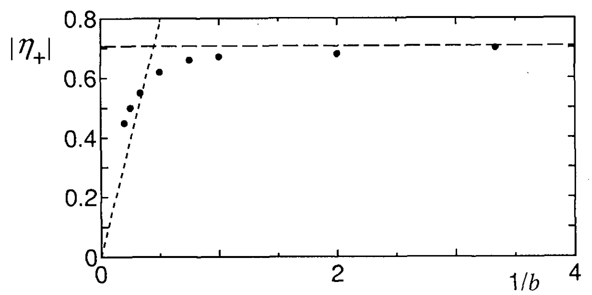

Fig. 8 The change in the depression $|\eta_+|$ with varying $1/b$. $\Gamma = 0$. Dashed line is the approximated solution for $b \ll 1$, dotted line for $b \gg 1$.

as the products of the velocities of steady state jumps and the elapsed time. We can see both lines agree well with each other above the topography and for downstream depression. The reason is because the effect of dispersion is not significant there. On the upstream side of the topography, the solitary waves are emitted very close to the topography so the above analytical model is not adequate in this part. **Figure 6 (b)** is the case of $\Gamma = 3$: large Γ. As stated above, the information of the disturbance to the downstream side is not obtained in the analytical study. Concerning with the hump above the topography, a little difference in height can be seen. The discrepancy becomes larger as b increases. So it can be said that the dispersion affect the behavior near the topography for large Γ.

Next a part of the profile is examined in detail. **Figure 7** shows the dependence of η_+ on small Γ for $b = 0.3$. We can see good agreement between the numerical result and analytical (dashed line, see (6)) one for $\Gamma > 0$. When Γ is negative, the numerical results divert from the analytical line. As in this case the downstream solitary wave train continues to stay very close to the topography, the uniform depression near the topography is not clear. So the analytical study without dispersion is not adequate.

Table 1 The value of Γ_+ for various b. The remarkable change in wave field occurs at $\Gamma = \Gamma_+$.

b	Γ_+
0.3	2.45 ± 0.05
1.0	1.95 ± 0.05
2.0	1.75 ± 0.05
5.0	0.95 ± 0.05

The change of η_+ with steepness of the topography b is also investigated. The result for $\Gamma = 0$ is shown in **Fig. 8**. For $b \ll 1$ (*i.e.* $1/b \gg 1$) very good agreement with the analytical result can be seen. The analytical approximation explains roughly the numerical result. However, for $b \gg 1$, there is a discrepancy between the analytical result and the numerical one. One reason for it is that as b increases, the value of η_+ comes to be unclear due to the disturbance emitted downstream associated with the emission of a solitary weve upstream (see **Fig. 5**). Even this effect is taken into account, the error is not so small. Improvement of the analytical approximation for $b \gg 1$ is required.

Finally we comment on a critical value of Γ, Γ_+. It is the value of Γ corresponding to the change of the wave field from the type of **Fig. 3** to that of **Fig. 4**. That is, for $\Gamma > \Gamma_+$ there is no solitary wave propagating upstream. **Table 1** shows the values of Γ_+ for some values of b. As b decreases Γ_+ approaches to the analytical value $2\sqrt{2} \simeq 2.828$ for $b \ll 1$ (see (6) or (7)). The deviation from the theoretical resultcan be seen for $b \gg 1$; $2\pi/b \simeq 1.26$ for $b = 5$ (see (9) or (10)).

4. Conclusion

The fBO equation is numerically solved to investigate the generation and propagation in the resonant flow. Not only the wave field itself but also the change of wave pattern depending on the Froude number is clarified. The comparison with analytical approximation shows essentials of the equation. In particular, it is found how the dispersive effect works by means of comparison with the dispersionless solution.

There is a limitation of the fBO equation, that is, the topography is required to be very small in order for the wave amplitude to be small $(\beta \sim \epsilon^2)$. Concerning with this problem, Choi and Cammasa[8] recently derived the equations describing the non-small amplitude waves in two-layer fluid without topography. The investigation of non-small amplitude wave motion is now in progress using this equation including the topographic effect. The result will be reported in near future.

Reference

1) R. Grimshaw and N. Smyth: J. Fluid Mech. **169** (1986) 429.
2) W. Melville and K. Helfrich: J. Fluid Mech. **178** (1987) 31.
3) T. Benjmain: J. Fluid Mech. **29** (1967) 559.
4) H. Ono: J. Phys. Soc. Japan **39** (1975) 1082.
5) Y. Matsuno: Phys. Rev. E**52** (1995) 6333.
6) R. Grimshaw: J. Phys. Oceanogr. **17** (1987) 53.
7) S. Wineberg, J. McGraph, E. Gabl and L. Scott: J. Comp. Phys. **97** (1991) 311.
8) W. Choi and R. Camassa: Phys. Rev. Lett. **77** (1996) 1759.